

1

## 2 Title page

3

4 A Novel Angiogenesis Role of GLP-1(32-36) to Rescue Diabetic Ischemic Lower Limbs  
5 via GLP-1R-Dependent Glycolysis  
6 GLP-1(32-36) Promotes Angiogenesis by GLP-1R-Dependent Glycolysis

7

## 8 Authors

9 Yikai Zhang<sup>1†</sup>, Shengyao Wang<sup>1†</sup>, Qiao Zhou<sup>1</sup>, Yepeng Hu<sup>1</sup>, Yi Xie<sup>1</sup>, Weihuan Fang<sup>3</sup>,  
10 Changxin Yang<sup>1</sup>, Zhe Wang<sup>1</sup>, Shu Ye<sup>1</sup>, Xinyi Wang<sup>2</sup>, Chao Zheng<sup>1,2\*</sup>

11

## 12 Affiliations

13 <sup>1</sup> Department of Endocrinology, The Second Affiliated Hospital, School of Medicine,  
14 Zhejiang University, Hangzhou, Zhejiang, China.

15 <sup>2</sup> Department of Endocrinology, The Second Affiliated Hospital and Yuying Children's  
16 Hospital of Wenzhou Medical University, Wenzhou, Zhejiang, China.

17 <sup>3</sup> Department of Veterinary Medicine, Zhejiang University, Hangzhou, Zhejiang, China

18

19

20 \*Address correspondence to: Chao ZHENG, E-mail: chao\_zheng@zju.edu.cn.

21

22 †These authors share the first authorship.

23

24

25

26

27

28

29

30

31

32

33

34

35

36

37

38

39

40

41

42

43

44

45

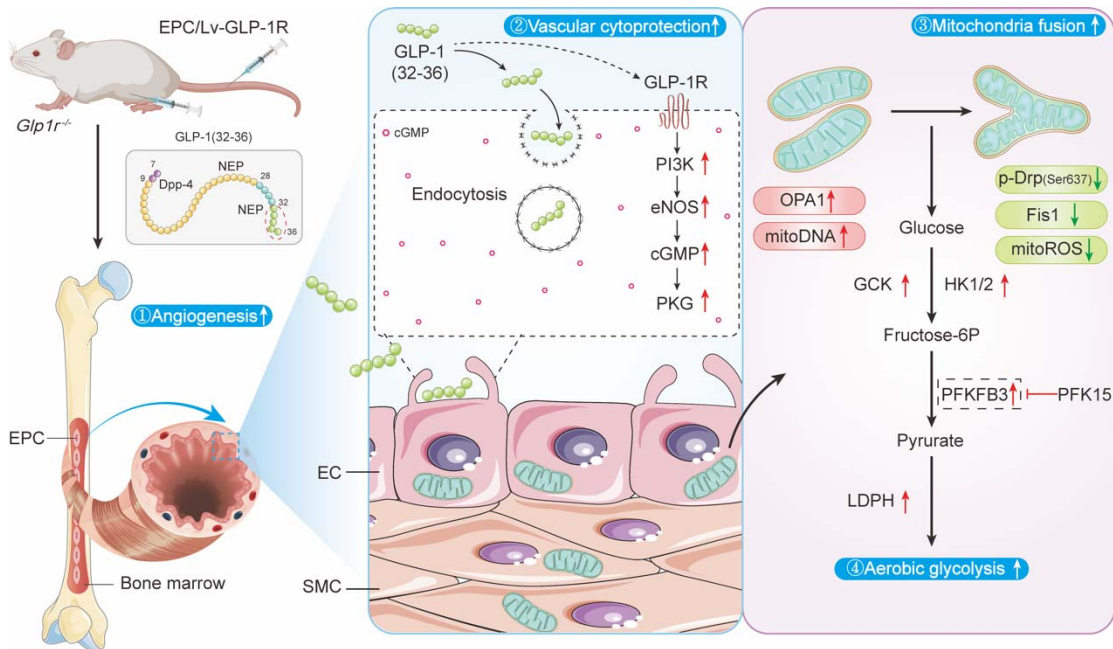
46

47

48 **Abstract**

49 Glucagon-like peptide 1 (GLP-1) improves angiogenesis, but the mechanism remains unclear. To  
50 address this question, we conducted a metabolomics analysis in bone marrow-derived endothelial  
51 progenitor cells (EPCs) isolated from T1DM mice treated with or without GLP-1(32-36) amide,  
52 an end-product of GLP-1. GLP-1(32-36) treatment recovered glycolysis. In addition, GLP-1(32-  
53 36) treatment rescued diabetic ischemic lower limbs and EPCs dysfunction by regulating  
54 PFKFB3-driven glycolytic flux capacity and mitochondrial dynamics. The effects of GLP-1(32-  
55 36) were abolished in mice lacking a functional GLP-1 receptor (*Glp1r*<sup>-/-</sup>), which could be  
56 partially rescued in EPCs transiently expressing GLP-1R. GLP-1(32-36) treatment activated the  
57 eNOS/cGMP/PKG pathway, increased glycolysis, and enhanced EPCs angiogenesis. Taken  
58 together, these findings suggest that GLP-1(32-36) could be used as a monotherapy or add-on  
59 therapy with existing treatments for DPAD.

60 **Graphical abstract**



61  
62  
63  
64  
65  
66  
67  
68  
69  
70  
71  
72  
73  
74

75 **MAIN TEXT**

76 **1. Introduction**

77 Peripheral arterial disease (PAD), a severe chronic complication of diabetes, is  
78 characterized by the narrowing and occlusion of arteries supplying the lower extremities  
79 (1). Although PAD typically presents as claudication, it can progress to critical limb  
80 ischemia and may eventually require amputation (2). Given that diabetic patients are at a  
81 fourfold greater risk of developing PAD than the general population, there is likely a close  
82 relationship between hyperglycemia and vascular complications (3). Recent studies reveal  
83 that incretins such as glucagon-like peptide 1 (GLP-1) play a role in modulating  
84 angiogenesis beyond their function in glycemic control (4, 5).

85 GLP-1 is a naturally occurring hormone that plays a vital role in regulating glucose  
86 homeostasis by stimulating insulin secretion (6). It is produced by enteroendocrine L cells  
87 located in the distal ileum and colon, and is found in two molecular forms, GLP-1 (7-37)  
88 and GLP-1 (7-36) amide, which bind to a specific G-protein coupled receptor called GLP-  
89 1R (7, 8). However, they are rapidly degraded by the enzyme dipeptidyl peptidase-4  
90 (DPP-4) after their release into the bloodstream, resulting in the formation of amino-  
91 terminally truncated peptides, such as GLP-1(9-37) and GLP-1(9-36) amide (9). GLP-1(9-  
92 36) amide can enter cells by penetrating the cell membrane, where it is internally cleaved  
93 in the C-terminal region by an intracellular endopeptidase such as neutral endopeptidase  
94 24.11 (NEP 24.11), leading to the production of the nonapeptide GLP-1 (28-36) and the  
95 pentapeptide GLP-1(32-36) amide (10) (Fig. 1A).

96 Several GLP-1 peptides and their metabolites are reported to have a cardiovascular  
97 protective effect. For example, GLP-1(9-36) has been shown to improve human aortic  
98 endothelial cell viability in response to hypoxia via a NO-dependent mechanism (11).  
99 GLP-1(9-36) has also been found to reduce high glucose-induced mitochondrial ROS  
100 generation in human endothelial cells (12). GLP-1(28-36) activates the AC-cAMP  
101 signaling pathway, changes the metabolic status of vascular cells, and plays a role in  
102 cardiovascular protection (13). GLP-1 (32-36), the major end-product of GLP-1  
103 proteolysis in addition to the nonapeptide, has been found to decrease body weight,  
104 increase energy consumption, and reduce  $\beta$ -cell apoptosis in obese mice (14, 15).  
105 However, whether GLP-1 (32-36) has a beneficial effect on diabetic vascular endothelial  
106 injury remains unclear.

107 By binding to its receptor (GLP-1R) expressed in various organs, including  
108 pancreatic islets, heart, lungs, and brain stem, GLP-1 activates the cAMP-dependent signal

109 transduction pathway to promote glucose-dependent insulin secretion by  $\beta$ -cells and  
110 improve nutrient utilization in peripheral organs (16). While GLP-1 metabolites have been  
111 found to exert beneficial effects when administered parenterally, their mechanisms of  
112 action are not fully understood (17-20). GLP-1 has been shown to protect against heart  
113 failure through the GLP-1R-mediated eNOS/cGMP/PKG pathway rather than the  
114 cAMP/PKA pathway (21). The mode of GLP-1(32-36) entry and its possible signaling  
115 mechanisms, if ever exist, remain unknown.

116 It has been proposed that endothelial cells (ECs) play a critical role in maintaining  
117 vascular homeostasis and promoting angiogenesis by relying on glycolysis to produce  
118 more than 80% of their ATP (22-24). A recent study suggests that GLP-1 can regulate  
119 astrocytic glycolysis, which may contribute to its neuroprotective effects in Alzheimer's  
120 disease (25). Therefore, it is reasonable to hypothesize that GLP-1(32-36) may enhance  
121 glycolytic flux in ECs, thereby altering vessel sprouting and promoting angiogenesis.

122 In this study, we demonstrate that GLP-1(32-36) administration has a direct effect on  
123 diabetic lower limb ischemia. We also demonstrate that GLP-1(32-36) has a causal role in  
124 improving fragile mitochondrial function and metabolism via the GLP-1R-mediated  
125 pathway, independent of its insulinotropic action. Specifically, we found that GLP-1(32-  
126 36) promotes angiogenesis in endothelial progenitor cells (EPCs) exposed to high glucose  
127 and enhances blood perfusion in ischemic tissues in STZ-induced type 1 diabetic mice  
128 with hindlimb ischemia (HLI). We also show that GLP-1(32-36) improves mitochondrial  
129 dynamics and rescues glycolysis mediated by 6-phosphofructo-2-kinase/fructose-2,6-  
130 bisphosphatase 3 (PFKFB3). We further demonstrate that GLP-1(32-36) rescues diabetic  
131 ischemic lower limbs by activating the GLP-1R-dependent eNOS/cGMP/PKG pathway.  
132 Our findings provide novel insights into the mechanisms underlying the beneficial effects  
133 of GLP-1(32-36) on DPAD and highlight its potential therapeutic value for non-diabetic  
134 patients due to its angiogenic effect that is independent of insulin regulation.

## 135 2. Results

### 136 2.1 GLP-1 (32-36) promotes blood perfusion and angiogenesis post-HLI in type 1 137 diabetic mice independent of insulinotropic actions.

138 We found that GLP-1(32-36) treatment protected human umbilical vein endothelial  
139 cells (HUVECs) from high glucose (HG)-induced reduction in tuber formation  
140 (Supplementary Fig. 1), indicating improved HUVEC integrity and function. Unlike GLP-  
141 1(7-36), GLP-1(32-36) does not stimulate insulin secretion from insulinoma 1 (INS-1) cell  
142 under either high or low glucose conditions, suggesting that the angiogenic capability of

143 this pentapeptide is independent of insulinotropic action (Fig. 1B). To investigate whether  
144 GLP-1(32-36) promotes angiogenesis in vivo, we used STZ-induced type 1 diabetic mice  
145 (T1DM) as a murine model of unilateral hind limb ischemia (HLI) to examine the  
146 therapeutic potential of GLP-1(32-36) on angiogenesis according to previous protocols  
147 (26-28) (Supplemental Fig. 2). The mice were treated with GLP-1(32-36) (1 $\mu$ mol/kg/d),  
148 GLP-1(7-36) (1 $\mu$ mol/kg/d), or PBS by daily intraperitoneal (i.p.) infusion and the blood  
149 flow recovery was evaluated by using a PeriCam Perfusion Speckle Imager (PSI) at day 0,  
150 3, 7, 14, 21, 28 days after HLI surgery (Supplementary Table. 1). GLP-1(7-36) here was  
151 used as a control for angiogenic drug (28). GLP-1(32-36) treatment markedly recovered  
152 blood flow, accompanied with improved neovascularization in ischemic tissue (Fig. 2A).  
153 The effect of the pentapeptide in promoting neovascularization was characterized by  
154 enhanced CD31 expression in ischemic gastrocnemius muscle, as shown by Western  
155 blotting and immunofluorescence staining (Fig. 2B-E). To investigate the effect of GLP-  
156 1(32-36) on EPC mobilization in response to tissue ischemia, we examined the numbers of  
157 double positive Sca-1 $^{+}$ /Flk-1 $^{+}$  cells in mononuclear fraction of peripheral blood from  
158 T1DM mice by flow cytometry. Administration of GLP-1(32-36) into tissue ischemia  
159 T1DM mice substantially augmented EPC mobilization on day 3 and peaked on day 7  
160 after HLI (Fig. 2F-G). These results demonstrate that GLP-1(32-36) is superior to GLP-  
161 1(7-36) in rescuing angiogenic function and blood perfusion in ischemic limb of STZ-  
162 induced diabetic mice without an effect on insulin secretion.

163 **2.2 GLP-1(32-36) protects mitochondria from high glucose-induced damage by**  
164 **enhancing glycolytic metabolism**

165 Endothelial metabolism plays an important role in regulating angiogenesis and  
166 mitochondrial membrane remodeling is highly responsive to changes in cell  
167 metabolism(29). As EPCs are considered to control the angiogenic switch of many  
168 physiological and pathologic processes, such as neovascularization (30), we assessed  
169 whether GLP-1(32-36) plays a role in improving angiogenesis by regulating mitochondrial  
170 dynamics and metabolism. Mice primary bone marrow EPCs (mEPCs) from T1DM mice  
171 or T1DM mice injected with GLP-1(32-36) were isolated and cultured, and the 3- to 5-  
172 passage mEPCs were used for further experiments. (Supplementary Figure 3).  
173 Ultrastructure examination revealed significant increase in elongated mitochondria of  
174 mEPCs from STZ-induced diabetic mice treated with GLP-1(32-36), whereas  
175 mitochondria from diabetic mice were mostly round or circular (Fig. 3A, B). HG-  
176 stimulated accumulation of mitochondrial ROS and loss of mtDNA content were

177 suppressed by GLP-1(32-36) treatment (Fig. 3C, D). GLP-1(32-36) also reversed the  
178 effect of HG on mitochondrial membrane potential as well as basal and maximal oxygen  
179 consumption rate (OCR) in EPCs from T1DM mice (Fig. 3E-H).

180 By metabolomic analysis, we observed that GLP-1(32-36) treatment induced a  
181 compensatory increase in glycolysis in mEPCs from T1DM mice as demonstrated by  
182 increased glycolytic metabolites such as L-lactate, D-fructose 1,6-bisphosphate (FDP),  
183 dihydroxyacetone phosphate (DHAP), and phosphoenolpyruvate (PEP) (Fig. 4A-B). Eight  
184 of the ten genes involved in the aerobic glycolytic pathway were significantly up-  
185 regulated by GLP-1(32-36) (Supplementary Table 2, Fig. 4C), including PFKFB3 (6-  
186 phosphofructo-2-kinase/fructose-2,6-bisphosphatase 3) which is engaged in the rate-  
187 limiting step in glycolysis for increased pyruvate production. The extra pyruvate generated  
188 could be directed to lactate rather than to the TCA cycle by upregulation of Lactate  
189 dehydrogenase A (LDHA) (Fig. 4D). Seahorse assay also confirmed that GLP-1(32-36)  
190 enhanced glycolytic flux (extracellular acidification rate [ECAR]) (Fig. 4E-F). These data  
191 demonstrate that GLP-1(32-36) may ameliorate HG-induced excessive mitochondrial  
192 fission by resorting to aerobic glycolysis.

### 193 **2.3 GLP-1(32-36) improves angiogenesis via PFKFB3-mediated glycolysis.**

194 As PFKFB3 is a well-known glycolytic activator(31), we explored whether PFKFB3  
195 is required for the therapeutic function of GLP-1(32-36) in preventing EPCs angiogenesis  
196 disorder. mEPCs were treated with GLP-1(32-36), followed with the PFKFB3-specific  
197 inhibitor PFK15 (32) for 30 min. GLP-1(32-36) treatment remarkably upregulated  
198 PFKFB3 protein levels and the phosphorylated form of eNOS, which was suppressed by  
199 PFK15 treatment (Fig. 5A-C). PFK15 treatment also suppressed GLP-1(32-36)-induced  
200 NO secretion, tube formation, and migration area of EPCs (Fig. 5D-F). Taken together,  
201 these findings suggest that GLP-1(32-36) recuperates angiogenesis by activating PFKFB3-  
202 mediated glycolysis.

### 203 **2.4 GLP-1R is required for angiogenetic function of GLP-1(32-36).**

204 To test whether GLP-1R deletion interrupts GLP-1(32-36)-induced  
205 neovascularization in T1DM, we established *Glp1r* knockout mice (*Glp1r*<sup>-/-</sup> mice) by the  
206 CRISPR/Cas9 technology (Supplementary Fig 4, 5, Fig. 6A). The *Glp1r*<sup>-/-</sup> mice were  
207 allocated into four groups and one group infused with  $1 \times 10^6$  mBM-EPCs overexpressing  
208 GLP-1R (Ad-GLP-1R) or the Lv-NC control lentiviral vector via tail vein injection  
209 (Supplementary Fig 6). GLP-1(32-36) treatment had marginal effect on blood perfusion in  
210 the *Glp1r*<sup>-/-</sup> mice and those receiving control lentivirus (EPCs/Lv-NC), but time-

dependently increased blood perfusion in mice received EPCs/Ad-GLP-1R from day 3 to 21 after transplantation (Fig. 6B-C). The benefit of EPC/Ad-GLP-1R was demonstrated by increased expression of CD31, an endothelial cell marker, in ischemic gastrocnemius muscle measured 28 days after HLI (Fig. 6D-E). These findings indicate that GLP-1(32-36)-mediated angiogenesis in T1DM mice after HLI is dependent on GLP-1R expression.

## 2.5 GLP-1R binds to, but is not required for, GLP-1(32-36) entry into endothelial progenitor cells.

To address the question whether GLP-1(32-36) undergoes cellular uptake via GLP-1R, a Cy5-tagged GLP-1(32-36) probe (Cy5-GLP-1(32-36)) was used for fluorescent tracing (Supplementary Table 1, Supplementary Fig 7). Confocal imaging showed that Cy5-GLP-1(32-36) entered EPCs with the strongest intracellular signals observed within 30 min (Supplementary Fig 8). Interestingly, while treating the cells with endocytosis inhibitor Dyngo-4A almost completely blocked abrogate Cy5-GLP-1(32-36) internalization, deletion of GLP-1R had no significant effect on Cy5-GLP-1(32-36) entry into the cells, implicating that GLP-1(32-36) penetration is independent of GLP-1R (Fig. 7A-B).

To determine binding to GLP-1R is necessary for the angiogenetic effect of GLP-1(32-36), we conducted an affinity pull-down experiment with biotinylated GLP-1(32-36) (BIOT (32-36)) (Supplementary Table 3). In agreement with the finding of others (33), we found that the pentapeptide bound to GLP-1R (Fig. 7C). Global docking analysis revealed that GLP-1(32-36) bound to the GLP-1 binding site of GLP-1R for all crystal structures (Figure 7D-F). These data suggest that interaction with GLP-1R, though is not involved in GLP-1(32-36) entry into the cells, is required for activation of GLP-1R-mediated pathway to play its subsequent angiogenetic effect.

## 2.6 GLP-1(32-36) exerts its angiogenetic effect through the eNOS/cGMP/PKG pathway via GLP-1R

Human EPCs (hEPCs) were isolated from cord blood for its richness in EPCs (34), cells were isolated and identified by specific EPCs markers as previously described (35) (Supplementary Fig. 9). We found that GLP-1(32-36) increased generation of cGMP but not cAMP (Supplementary Fig 10), indicating that the pentapeptide might activate the eNOS/cGMP/PKG pathway to exert angiogenesis. Downregulation of GLP-1R by siRNA silencing attenuated GLP-1(32-36)-induced cGMP increase and NO formation (Supplementary Fig. 6B; Fig. 8A-B). Suppressing GLP-1R also recued GLP-1(32-36)-stimulated p-eNOS and PKG expression (Fig. 8C-E). GLP-1(32-36) treatment resecured

245 HG-induced impairment in tube formation and migration, but this effect was suppressed  
246 by GLP-1R downregulation (Fig. 8E-F). These data uncover a mechanism whereby GLP-  
247 1(32-36) improves angiogenesis in HG-exposed EPCs.

248 **2.7 GLP-1R is involved in mitochondrial dynamics and GLP-1(32-36)-mediated**  
249 **glycolysis.**

250 We examined the potential effect of GLP-1(32-36) on mitochondrial biogenesis in  
251 EPCs treated the GLP-1R antagonist (exendin (9-39)). GLP-1(32-36) recovered the  
252 mitochondrial morphology, which is blocked by exendin (Supplementary. 11A-E).  
253 Inhibition of GLP-1R also interrupted the improvement of MMP and mitochondrial OCR  
254 level by pentapeptide (Supplementary. 11F-I). These results suggest that GLP-1R is  
255 involved in pentapeptide-mediated mitochondrial homeostasis.

256 Given that PFKFB3 plays an important role in vessel sprouting by promoting  
257 glycolysis(31), we wondered if GLP-1R is involved in GLP-1(32-36)-mediated effects on  
258 metabolism. Suppressing GLP-1R by shRNA impaired ATP turnover, abolished the  
259 positive effect of GLP-1(32-36) on lactate accumulation (Fig. 9A-B), and blocked the  
260 effect of GLP-1(32-36) on glucose uptake (Fig. 9C-D). More importantly, downregulation  
261 of GLP-1R suppressed PFKFB3 expression (Fig. 9E-F). These data reveal that GLP-1R is  
262 responsible for GLP-1(32-36)-mediated glycolysis via PFKFB3.

263 **3. Discussion**

264 GLP-1(9-36) is known to improve hypoxia-impaired human aortic endothelial cell  
265 viability (11) and attenuate HG-triggered mitochondrial ROS generation in human  
266 endothelial cells (12). Of the two peptides cleaved from GLP-1(9-36) amide by NEP  
267 24.11(10), GLP-1(28-36) could activate the AC-cAMP signaling pathway and play a role  
268 in cardiovascular protection (13) and GLP-1 (32-36) may increase energy consumption,  
269 decrease body weight and decrease  $\beta$ -cell apoptosis in obese mice (14, 15). However, if  
270 and how GLP-1(32-36) contributes to protection of vascular endothelial injury remains  
271 unexplored. Using in vivo, ex vivo and in vitro models, we demonstrate that GLP-1(32-  
272 36) is effective in rescuing angiogenic function, blood perfusion and promoted EPC  
273 mobilization in ischemic limb of STZ-induced diabetic mice independent of insulin  
274 release. Mechanistically, it recuperates angiogenesis by activating PFKFB3-mediated  
275 aerobic glycolysis and ameliorate excessive mitochondrial fission. Its interaction with  
276 GLP-1R is required for regulation of the glycolytic effect via PFKFB3 as well as for  
277 modulation of the eNOS/cGMP/PKG pathway to improve angiogenesis in high glucose-  
278 exposed EPCs. This study explores the mechanism by which GLP-1(32-36) promotes

279 angiogenesis and establishes the theoretical basis for the clinical development and  
280 application of angiogenic agents in diabetic foot patients.

281 PFKFB3 plays important roles in angiogenesis in several cell types (31). In cancer-  
282 associated fibroblasts and tumor endothelial cells, PFKFB3 is known to modulate  
283 angiogenesis via activation of the aerobic glycolysis, and blockade of PFKFB3 reduces  
284 tumor angiogenesis(36), while its expression is increased markedly in beta cells from type  
285 1 diabetes patients as well as in human and rat islets exposed to cytokines(37), and in  
286 kidneys from diabetic mice(38). Transcriptionally, PFKFB3 expression is regulated  
287 negatively by PGC1 $\alpha$ (39, 40) or Kruppel-like factor 2 (KLF2)(41), but positively by HIF-  
288 1 $\alpha$  in response to hypoxia(42, 43) . HIF1 $\alpha$  itself could be activated by ROS (44) or  
289 endothelial cell-sourced NO in astrocytes(45). Because GLP-1(32-36) increased PFKFB3  
290 without affecting cAMP in HG-exposed EPCs, and PGC1 $\alpha$  negatively regulates PFKFB3,  
291 it is less likely that the pentapeptide acts via the GLP-1R/cAMP/AMPK/PGC1 $\alpha$   
292 pathway(40, 46). Activation of HIF1 $\alpha$ -PFKFB3 axis is believed to divert glucose  
293 metabolism in diabetic  $\beta$ -cells away from mitochondria for glycolysis(44). Therefore, we  
294 propose that GLP-1(32-36) exerts its pro-angiogenetic effect in the EPCs exposed to high  
295 glucose by activating PI3K/eNOS/cGMP/PKG pathway with enhanced glycolysis and  
296 improved mitochondrial homeostasis via PFKFB3 upregulation. This is based on the facts  
297 that GLP-1(32-36) could derepress a series of molecules PI3K, NO/eNOS, cGMP and  
298 PKG which are involved in myocardial ischemic preconditioning(47), and increase  
299 expression of PFKFB3 possibly via NO activation of HIF1 $\alpha$  (44) leading to  
300 glucometabolic reprogramming shown as diversion of pyruvate away from  
301 mitochondria(40, 43).

302 GLP-1 is known to exert its effect through the unique GLP-1R in stimulating  
303 adenylate cyclase activity, and the resultant accumulation cyclic AMP (cAMP) leads to  
304 activation of protein kinase A (PKA), one of the multiple intracellular mediators in  
305 various tissue (48, 49). According to the “dual receptor theory” (16), GLP-1 may exert  
306 insulin mimetic actions on insulin-sensitive target tissues either by acting on GLP-1R to  
307 activate the pro-survival cAMP/PKA and PI3K/Akt pathways (49) or through an  
308 alternative mechanism independent of GLP-1R as seen with GLP-1(9-36) through a novel  
309 receptor/transporter(11, 16, 18). However, whether GLP-1R is involved in cellular uptake  
310 and activities of GLP-1(32-36), a further cleavage product derived from GLP-1(7-36) and  
311 GLP-1(9-36), has not been determined. We show that cellular entry of GLP-1(32-36) was

312 not affected by silencing of GLP-1R, but completely blocked by the dynamin inhibitor,  
313 suggesting that the pentapeptide enters the cell via endocytosis, as with most of the  
314 peptide hormones (33). By affinity pull-down and molecular docking analysis, we found  
315 that GLP-1R, though not required for GLP-1(32-36) uptake, might act as the binding  
316 partner.

317 Endothelial dysfunction in association with cGMP-NO insufficiency has been well  
318 established as an important correlate of heightened cardiovascular risk (50). NO is short-  
319 lived and acts in autocrine and paracrine manners by elevating cGMP/PKG, thereby  
320 exerting cardioprotective effects on remodeling(51). NO synthase null mutant mice  
321 displayed markedly reduced mitochondrial content associated with significantly lower  
322 oxygen consumption and ATP content(52). We hypothesized that GLP-1(32-36) might  
323 mediate eNOS/cGMP/PKG-dependent mitochondrial biogenesis to promote angiogenesis  
324 via GLP-1R. In our study, GLP-1(32-36) stimulated cGMP (but not cAMP) production,  
325 promoted NO release, eNOS phosphorylation and PKG expression, and enhanced tube  
326 formation and migration, all of which were suppressed by downregulation of GLP-1R.  
327 These data support a mechanism whereby GLP-1(32-36) utilizes GLP-1R to modulate the  
328 eNOS/cGMP/PKG pathway, independent of G-protein signaling, to play its roles in  
329 angiogenesis and glycolysis.

330 In addition, eNOS-derived NO is well known to tightly regulate mitochondrial  
331 functioning. In physiological concentrations, NO regulates mitochondrial network fusion  
332 by phosphorylating and inhibiting dynamin related GTPase (DRP1) through the sGC/PKG  
333 pathway(53). Our data also define the molecular mechanism of mitochondrial dynamics  
334 and metabolism mediated by GLP-1(32-36) through eNOS/cGMP/PKG pathway. Previous  
335 studies have showed that GLP-1 byproducts could target mitochondria upon entry into the  
336 cells. GLP-1(9-36) could reduce elevated levels of mitochondrial-derived ROS in  
337 Alzheimer's disease model mice(54). GLP-1(28-36) prevents ischemic cardiac injury by  
338 inhibiting mitochondrial trifunctional protein- $\alpha$ (13). It has been proposed that its C-  
339 terminal domain, VKGR amide, might contain a consensus mitochondrial targeting  
340 sequence(55). This suggests that GLP-1(32-36) might also play a role in regulating  
341 mitochondria fitness. We constructed Cy5-conjugated pentapeptide to visualize its  
342 internalization. Cy5-GLP-1(32-36) entered EPCs with the strongest intracellular signals  
343 observed within 30 min. Pharmacological inhibition of GLP-1R by chemical antagonists  
344 (exendin (9-39)) blunted peptides-regulated mitochondrial homeostasis and dynamics by  
345 tilting mitochondrial fission towards fusion. We found that GLP-1(32-36) rescues

346 mitochondrial morphology and protected oxidative stress injury from high glucose stress.  
347 These findings provide evidence that GLP-1(32-36) is involved in improvement of  
348 mitochondrial fitness.

349 Since endothelial function is intrinsically linked to its metabolism(56, 57). ECs are  
350 atypical nonmalignant cells that surprisingly depend on glycolysis to synthesize>80% of  
351 ATP even under well-oxygenated conditions(31, 58). We hypothesized that occurrence of  
352 PAD could be accompanied with metabolic abnormalities and failure to establish timely  
353 metabolic switch might negatively affect the function of endothelial cells. We investigated  
354 the metabolite profiles between mEPCs from T1DM with GLP-1(32-36) treatment and  
355 from control T1DM (without treatment). The results showed that high glucose stress  
356 resulted in glycolysis disorder which was rescued by GLP-1(32-36). Seahorse data also  
357 show that GLP-1(32-36) could improve basal and maximal respiration and glycolysis in  
358 mEPCs exposed to high glucose. Transcription of key genes involved in the aerobic  
359 glycolytic pathway and lactate level were increased by GLP-1(32-36) treatment. The  
360 elongated mature mitochondria of GLP-1(32-36)-treated EPCs and increased glycolysis,  
361 as opposed to immature round mitochondria lacking mature cristae characteristic of  
362 hyperglycemia, illustrates the importance of efficient biosynthetic organelles and efficient  
363 energy metabolism to support EPC proliferation required for angiogenesis.

364 Interestingly, we compared insulin secretion after treating GLP-1(7-36) and GLP-  
365 1(32-36) with different concentration. GLP-1(7-36) stimulates glucose-dependent insulin  
366 secretion, whereas GLP-1(32-36) has only weak partial insulinotropic agonist activities.  
367 This not only elucidates the key role of GLP-1R in the action of GLP-1(32-36) but also  
368 suggested GLP-1(32-36) has self-governed angiogenesis ability independent of insulin  
369 release and blood glucose control, expanding the possibility of the pentapeptide improving  
370 angiogenesis in non-diabetic patients.

371 In summary, we have found that GLP-1(32-36) functions in cooperation with GLP-  
372 1R in mediating eNOS-cGMP-PKG signaling, mitochondrial homeostasis and metabolic  
373 functions of endothelial cells in favor of angiogenesis. GLP-1(32-36) prevents HG-  
374 mediated mitochondrial fission, regulates metabolic reprogramming by enhanced PFKFB3  
375 expression and glycolysis, and improve EPCs angiogenesis. Our results are consistent with  
376 an emerging appreciation that GLP-1R mediated mitochondrial dynamics and energy  
377 metabolism plays a central role in endothelial angiogenesis. We believe that the  
378 mechanistic pathway uncovered here has potential impact, from the clinical perspective,  
379 on therapy of PAD, for which no approved therapies currently exist. GLP-1(32-36) may

380 offer supplementary protection against ischemic angiogenesis in instances where reduced  
381 blood flow-related mitochondrial fitness and glycolysis is compromised before apparent  
382 clinical manifestation.

#### 383 **4. Materials and Methods**

384 The origins and specifications of the mice used in this study are detailed in the  
385 Supplemental Methods. Descriptions of detailed methods of T1DM *in vivo* (26) and  
386 mouse HLI models *in vivo* (59) are provided in the Supplemental Methods. Details on the  
387 isolation of mEPCs and hEPCs, and cell culture methods, including drug treatment  
388 regimens, are provided in the Supplemental Methods. All assays relevant to cAMP,  
389 cGMP, and Seahorse XFe96 extracellular flux measurements are detailed. Gene silencing  
390 using siRNA and Western blotting protocols are described in the Supplemental  
391 Information.

#### 392 **4.1 Statistics**

393 Data are presented as mean  $\pm$  SEM. Comparisons between two groups were  
394 performed by Student's 2-tailed t test. Comparisons of data with three or more groups  
395 were performed using 1-way ANOVA with Tukey's post hoc multiple comparisons.  
396 Repeated-measures ANOVA was performed when appropriate. All statistical analyses  
397 were performed in GraphPad Prism (Version 9.0). In all cases, differences were  
398 considered significant at  $^*P < 0.05$  and highly significant at  $^{**}P < 0.01$  and  $^{***}P < 0.001$ ;  
399 ns means no significance.

#### 400 **4.2 Study approval**

401 Experimental setups and animal care were permitted by the Animal Policy and  
402 Welfare Committee of Zhejiang University (ethical approval code:2021-NO.172). And for  
403 human studies, the work was approved by the Ethics Committee of Zhejiang University  
404 (ethical approval code: 2021-NO.0318) and carried out in accordance with the Declaration  
405 of Helsinki. All participants gave written informed consent.

#### 406 **407 Author Contributions:**

408 Yikai Zhang<sup>†</sup>: Conceptualization, designing research studies and writing the  
409 manuscript, Shengyao Wang<sup>†</sup>: Conducting experiments, acquiring data and analyzing  
410 data. They shared first authorship. Qiao Zhou, Yepeng Hu and Yi Xie: Conducting  
411 experiments and analyzing data. Weihuan Fang: reviewing & editing the manuscript. Zhe  
412 Wang, Shu Ye and Xinyi Wang: Data curation. Chao Zheng<sup>\*</sup>: Supervision, administrating  
413 project and funding the study.

414  
415  
416  
417  
418  
419 **Funding**  
420  
421  
422  
423  
424  
425 **Conflicts of Interest**  
426  
427  
428  
429 **Supplementary Materials**  
430  
431  
432  
433 **Fig. S1.** GLP-1(32-36) improves angiogenesis of HUVECs in hyperglycemia.  
434 **Fig. S2.** Streptozotocin-induced diabetic models in Mice.  
435 **Fig. S3.** Characterization of isolated mice bone marrow EPCs.  
436 **Fig. S4.** *GLP1r* Cas9-KO strategy.  
437 **Fig. S5.** Diabetic model in *GLP-1*<sup>-/-</sup> with transplanting EPCs/Lv-GLP-1R or control.  
438 **Fig. S6.** Verification the effect of lentivirus overexpression in mBM-EPCs and hUCB-  
439 EPCs.  
440 **Fig. S7.** Synthesis of Cy5-GLP-1(32-36).  
441 **Fig. S8.** Cellular uptake of GLP-1(32-36).  
442 **Fig. S9.** Characterization of isolated human EPCs(hEPCs).  
443 **Fig. S10.** GLP-1(32-36) do not stimulate intracellular cAMP accumulation but cGMP in  
444 EPCs.  
445  
446 **Table S1.** Amino acid sequences of synthetic peptides used.

447 **Table S2.** List of primer sequences used for quantitative RT-PCR.

448 **Table S3.** Amino acid sequences of biotinylated peptides used.

449 **Table S4.** Lentivirus sequences to inhibit or overexpress gene expression.

450

## 451 **References**

- 452 1.Ungerleider JL, Christman KL. Concise Review: Injectable Biomaterials for the Treatment of  
453 Myocardial Infarction and Peripheral Artery Disease: Translational Challenges and Progress.  
454 Stem cells translational medicine. 2014;3(9):1090-9.
- 455 2.Klein AJ, Ross CB. Endovascular treatment of lower extremity peripheral arterial disease.  
456 Trends Cardiovasc Med. 2016;26(6):495-512.
- 457 3.Petznick AM, Shubrook JH. Treatment of specific macrovascular beds in patients with diabetes  
458 mellitus. Osteopath Med Prim Care. 2010;4:5.
- 459 4.Aronis KN, Chamberland JP, Mantzoros CS. GLP-1 promotes angiogenesis in human  
460 endothelial cells in a dose-dependent manner, through the Akt, Src and PKC pathways.  
461 Metabolism. 2013;62(9):1279-86.
- 462 5.Katare R, Riu F, Rowlinson J, Lewis A, Holden R, Meloni M, et al. Perivascular delivery of  
463 encapsulated mesenchymal stem cells improves postischemic angiogenesis via paracrine  
464 activation of VEGF-A. Arterioscler Thromb Vasc Biol. 2013;33(8):1872-80.
- 465 6.Phillips LK, Prins JB. Update on incretin hormones. Ann N Y Acad Sci. 2011;1243:E55-74.
- 466 7.Orskov C, Wettergren A, Holst JJ. Biological effects and metabolic rates of glucagonlike  
467 peptide-1 7-36 amide and glucagonlike peptide-1 7-37 in healthy subjects are indistinguishable.  
468 Diabetes. 1993;42(5):658-61.
- 469 8.Kieffer TJ, Habener JF. The glucagon-like peptides. Endocrine reviews. 1999;20(6):876-913.
- 470 9.Beinborn M, Worrall CI, McBride EW, Kopin AS. A human glucagon-like peptide-1 receptor  
471 polymorphism results in reduced agonist responsiveness. Regulatory peptides. 2005;130(1-2):1-6.
- 472 10.Hupe-Sodmann K, McGregor GP, Bridenbaugh R, Göke R, Göke B, Thole H, et al.  
473 Characterisation of the processing by human neutral endopeptidase 24.11 of GLP-1(7-36) amide  
474 and comparison of the substrate specificity of the enzyme for other glucagon-like peptides. Regul  
475 Pept. 1995;58(3):149-56.
- 476 11.Ban K, Kim KH, Cho CK, Sauvé M, Diamandis EP, Backx PH, et al. Glucagon-like peptide  
477 (GLP)-1(9-36)amide-mediated cytoprotection is blocked by exendin(9-39) yet does not require  
478 the known GLP-1 receptor. Endocrinology. 2010;151(4):1520-31.

479 12.Giacco F, Du X, Carratú A, Gerfen GJ, D'Apolito M, Giardino I, et al. GLP-1 Cleavage  
480 Product Reverses Persistent ROS Generation After Transient Hyperglycemia by Disrupting an  
481 ROS-Generating Feedback Loop. *Diabetes*. 2015;64(9):3273-84.

482 13.Siraj MA, Mundil D, Beca S, Momen A, Shikatani EA, Afroze T, et al. Cardioprotective GLP-  
483 1 metabolite prevents ischemic cardiac injury by inhibiting mitochondrial trifunctional protein- $\alpha$ .  
484 *J Clin Invest*. 2020;130(3):1392-404.

485 14.Tomas E, Stanojevic V, McManus K, Khatri A, Everill P, Bachovchin WW, et al. GLP-1(32-  
486 36)amide Pentapeptide Increases Basal Energy Expenditure and Inhibits Weight Gain in Obese  
487 Mice. *Diabetes*. 2015;64(7):2409-19.

488 15.Sun L, Dai Y, Wang C, Chu Y, Su X, Yang J, et al. Novel Pentapeptide GLP-1 (32-36) Amide  
489 Inhibits  $\beta$ -Cell Apoptosis In Vitro and Improves Glucose Disposal in Streptozotocin-Induced  
490 Diabetic Mice. *Chemical biology & drug design*. 2015;86(6):1482-90.

491 16.Tomas E, Habener JF. Insulin-like actions of glucagon-like peptide-1: a dual receptor  
492 hypothesis. *Trends Endocrinol Metab*. 2010;21(2):59-67.

493 17.Nikolaidis LA, Elahi D, Shen YT, Shannon RP. Active metabolite of GLP-1 mediates  
494 myocardial glucose uptake and improves left ventricular performance in conscious dogs with  
495 dilated cardiomyopathy. *Am J Physiol Heart Circ Physiol*. 2005;289(6):H2401-8.

496 18.Ban K, Noyan-Ashraf MH, Hoefer J, Bolz SS, Drucker DJ, Husain M. Cardioprotective and  
497 vasodilatory actions of glucagon-like peptide 1 receptor are mediated through both glucagon-like  
498 peptide 1 receptor-dependent and -independent pathways. *Circulation*. 2008;117(18):2340-50.

499 19.Tomas E, Wood JA, Stanojevic V, Habener JF. GLP-1-derived nonapeptide GLP-1(28-  
500 36)amide inhibits weight gain and attenuates diabetes and hepatic steatosis in diet-induced obese  
501 mice. *Regul Pept*. 2011;169(1-3):43-8.

502 20.Elahi D, Angeli FS, Vakilipour A, Carlson OD, Tomas E, Egan JM, et al. GLP-1(32-36)amide,  
503 a novel pentapeptide cleavage product of GLP-1, modulates whole body glucose metabolism in  
504 dogs. *Peptides*. 2014;59:20-4.

505 21.Chen J, Wang D, Wang F, Shi S, Chen Y, Yang B, et al. Exendin-4 inhibits structural  
506 remodeling and improves  $Ca(2+)$  homeostasis in rats with heart failure via the GLP-1 receptor  
507 through the eNOS/cGMP/PKG pathway. *Peptides*. 2017;90:69-77.

508 22.Eelen G, de Zeeuw P, Treps L, Harjes U, Wong BW, Carmeliet P. Endothelial Cell  
509 Metabolism. *Physiol Rev*. 2018;98(1):3-58.

510 23.Li X, Sun X, Carmeliet P. Hallmarks of Endothelial Cell Metabolism in Health and Disease.  
511 *Cell Metab*. 2019;30(3):414-33.

512 24.Li X, Kumar A, Carmeliet P. Metabolic Pathways Fueling the Endothelial Cell Drive. *Annu*  
513 *Rev Physiol.* 2019;81:483-503.

514 25.Zheng J, Xie Y, Ren L, Qi L, Wu L, Pan X, et al. GLP-1 improves the supportive ability of  
515 astrocytes to neurons by promoting aerobic glycolysis in Alzheimer's disease. *Mol Metab.*  
516 2021;47:101180.

517 26.Wu KK, Huan Y. Streptozotocin-induced diabetic models in mice and rats. *Curr Protoc*  
518 *Pharmacol.* 2008;Chapter 5:Unit 5.47.

519 27.Yu J, Dardik A. A Murine Model of Hind Limb Ischemia to Study Angiogenesis and  
520 Arteriogenesis. *Methods Mol Biol.* 2018;1717:135-43.

521 28.Yan X, Su Y, Fan X, Chen H, Lu Z, Liu Z, et al. Liraglutide Improves the Angiogenic  
522 Capability of EPC and Promotes Ischemic Angiogenesis in Mice under Diabetic Conditions  
523 through an Nrf2-Dependent Mechanism. *Cells.* 2022;11(23).

524 29.Mishra P, Chan DC. Metabolic regulation of mitochondrial dynamics. *J Cell Biol.*  
525 2016;212(4):379-87.

526 30.Gao D, Nolan DJ, Mellick AS, Bambino K, McDonnell K, Mittal V. Endothelial progenitor  
527 cells control the angiogenic switch in mouse lung metastasis. *Science.* 2008;319(5860):195-8.

528 31.De Bock K, Georgiadou M, Schoors S, Kuchnio A, Wong BW, Cantelmo AR, et al. Role of  
529 PFKFB3-driven glycolysis in vessel sprouting. *Cell.* 2013;154(3):651-63.

530 32.Zhu W, Ye L, Zhang J, Yu P, Wang H, Ye Z, et al. PFK15, a Small Molecule Inhibitor of  
531 PFKFB3, Induces Cell Cycle Arrest, Apoptosis and Inhibits Invasion in Gastric Cancer. *PLoS*  
532 *One.* 2016;11(9):e0163768.

533 33.Pandey KN. Endocytosis and Trafficking of Natriuretic Peptide Receptor-A: Potential Role of  
534 Short Sequence Motifs. *Membranes (Basel).* 2015;5(3):253-87.

535 34.Murohara T, Ikeda H, Duan J, Shintani S, Sasaki K, Eguchi H, et al. Transplanted cord blood-  
536 derived endothelial precursor cells augment postnatal neovascularization. *The Journal of clinical*  
537 *investigation.* 2000;105(11):1527-36.

538 35.Yan X, Cai S, Xiong X, Sun W, Dai X, Chen S, et al. Chemokine receptor CXCR7 mediates  
539 human endothelial progenitor cells survival, angiogenesis, but not proliferation. *Journal of*  
540 *cellular biochemistry.* 2012;113(4):1437-46.

541 36.Cantelmo AR, Conradi LC, Brajic A, Goveia J, Kalucka J, Pircher A, et al. Inhibition of the  
542 Glycolytic Activator PFKFB3 in Endothelium Induces Tumor Vessel Normalization, Impairs  
543 Metastasis, and Improves Chemotherapy. *Cancer Cell.* 2016;30(6):968-85.

544 37.Nomoto H, Pei L, Montemurro C, Rosenberger M, Furterer A, Coppola G, et al. Activation of  
545 the HIF1 $\alpha$ /PFKFB3 stress response pathway in beta cells in type 1 diabetes. *Diabetologia*.  
546 2020;63(1):149-61.

547 38.Song C, Wang S, Fu Z, Chi K, Geng X, Liu C, et al. IGFBP5 promotes diabetic kidney disease  
548 progression by enhancing PFKFB3-mediated endothelial glycolysis. *Cell Death Dis*.  
549 2022;13(4):340.

550 39.Prieto I, Alarcón CR, García-Gómez R, Berdún R, Urgel T, Portero M, et al. Metabolic  
551 adaptations in spontaneously immortalized PGC-1 $\alpha$  knock-out mouse embryonic fibroblasts  
552 increase their oncogenic potential. *Redox Biol*. 2020;29:101396.

553 40.Li X, Jiang E, Zhao H, Chen Y, Xu Y, Feng C, et al. Glycometabolic reprogramming-mediated  
554 proangiogenic phenotype enhancement of cancer-associated fibroblasts in oral squamous cell  
555 carcinoma: role of PGC-1 $\alpha$ /PFKFB3 axis. *Br J Cancer*. 2022;127(3):449-61.

556 41.Doddaballapur A, Michalik KM, Manavski Y, Lucas T, Houtkooper RH, You X, et al.  
557 Laminar shear stress inhibits endothelial cell metabolism via KLF2-mediated repression of  
558 PFKFB3. *Arterioscler Thromb Vasc Biol*. 2015;35(1):137-45.

559 42.Obach M, Navarro-Sabaté A, Caro J, Kong X, Duran J, Gómez M, et al. 6-Phosphofructo-2-  
560 kinase (pfkfb3) gene promoter contains hypoxia-inducible factor-1 binding sites necessary for  
561 transactivation in response to hypoxia. *J Biol Chem*. 2004;279(51):53562-70.

562 43.Min J, Zeng T, Roux M, Lazar D, Chen L, Tudzarova S. The Role of HIF1 $\alpha$ -PFKFB3 Pathway  
563 in Diabetic Retinopathy. *J Clin Endocrinol Metab*. 2021;106(9):2505-19.

564 44.Reichard A, Asosingh K. The role of mitochondria in angiogenesis. *Mol Biol Rep*.  
565 2019;46(1):1393-400.

566 45.Brix B, Mesters JR, Pellerin L, Jöhren O. Endothelial cell-derived nitric oxide enhances  
567 aerobic glycolysis in astrocytes via HIF-1 $\alpha$ -mediated target gene activation. *J Neurosci*.  
568 2012;32(28):9727-35.

569 46.Chen H, Fan W, He H, Huang F. PGC-1: a key regulator in bone homeostasis. *J Bone Miner  
570 Metab*. 2022;40(1):1-8.

571 47.Costa AD, Pierre SV, Cohen MV, Downey JM, Garlid KD. cGMP signalling in pre- and post-  
572 conditioning: the role of mitochondria. *Cardiovasc Res*. 2008;77(2):344-52.

573 48.Campbell JE, Drucker DJ. Pharmacology, physiology, and mechanisms of incretin hormone  
574 action. *Cell Metab*. 2013;17(6):819-37.

575 49.Baggio LL, Drucker DJ. Biology of incretins: GLP-1 and GIP. *Gastroenterology*.  
576 2007;132(6):2131-57.

577 50.Vita JA, Treasure CB, Nabel EG, McLenachan JM, Fish RD, Yeung AC, et al. Coronary  
578 vasomotor response to acetylcholine relates to risk factors for coronary artery disease. *Circulation*.  
579 1990;81(2):491-7.

580 51.Lee J, Bae EH, Ma SK, Kim SW. Altered Nitric Oxide System in Cardiovascular and Renal  
581 Diseases. *Chonnam Med J*. 2016;52(2):81-90.

582 52.Nisoli E, Falcone S, Tonello C, Cozzi V, Palomba L, Fiorani M, et al. Mitochondrial  
583 biogenesis by NO yields functionally active mitochondria in mammals. *Proc Natl Acad Sci U S*  
584 A. 2004;101(47):16507-12.

585 53.De Palma C, Falcone S, Pisoni S, Cipolat S, Panzeri C, Pambianco S, et al. Nitric oxide  
586 inhibition of Drp1-mediated mitochondrial fission is critical for myogenic differentiation. *Cell*  
587 *Death Differ*. 2010;17(11):1684-96.

588 54.Ma T, Du X, Pick JE, Sui G, Brownlee M, Klann E. Glucagon-like peptide-1 cleavage product  
589 GLP-1(9-36) amide rescues synaptic plasticity and memory deficits in Alzheimer's disease model  
590 mice. *J Neurosci*. 2012;32(40):13701-8.

591 55.Tomas E, Stanojevic V, Habener JF. GLP-1-derived nonapeptide GLP-1(28-36)amide targets  
592 to mitochondria and suppresses glucose production and oxidative stress in isolated mouse  
593 hepatocytes. *Regulatory peptides*. 2011;167(2-3):177-84.

594 56.Bierhansl L, Conradi LC, Treps L, Dewerchin M, Carmeliet P. Central Role of Metabolism in  
595 Endothelial Cell Function and Vascular Disease. *Physiology (Bethesda)*. 2017;32(2):126-40.

596 57.Eelen G, de Zeeuw P, Simons M, Carmeliet P. Endothelial cell metabolism in normal and  
597 diseased vasculature. *Circ Res*. 2015;116(7):1231-44.

598 58.Davidson SM, Duchen MR. Endothelial mitochondria: contributing to vascular function and  
599 disease. *Circ Res*. 2007;100(8):1128-41.

600 59.Limbourg A, Korff T, Napp LC, Schaper W, Drexler H, Limbourg FP. Evaluation of postnatal  
601 arteriogenesis and angiogenesis in a mouse model of hind-limb ischemia. *Nat Protoc*.  
602 2009;4(12):1737-46.

603

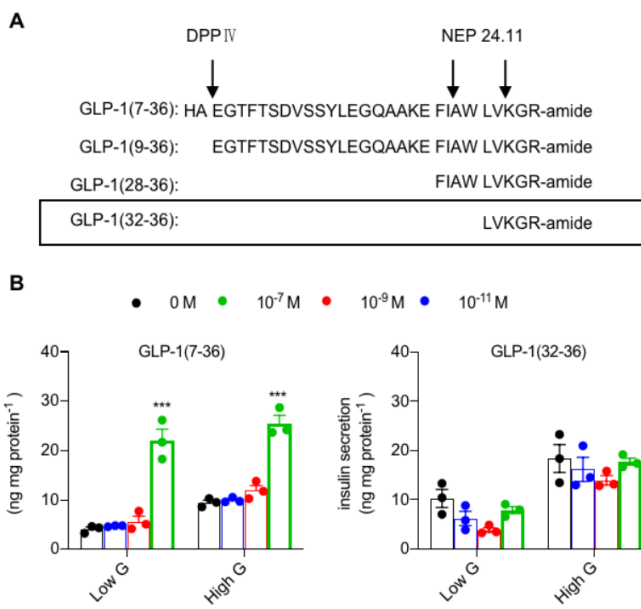


**Figure 1: GLP-1 metabolites influent different dose glucose-stimulated insulin secretion of INS-1 cells.** (A)Formation of the C-terminal peptides GLP-1(7-36), GLP-1(9-36), GLP-1(28-36), and GLP-1(32-36) amides. (B) INS-1 cells were treated with either GLP-1(7-36) or GLP-1(32-36) with different dose (0 M, 10<sup>-11</sup> M, 10<sup>-9</sup> M, 10<sup>-7</sup> M), and 48 h later, insulin secretion was measured under low glucose (2 mM) or high glucose (33 mM) concentrations. Cells were equilibrated with KRBB buffer and stimulated with 2.8 mM, 20 mM glucose and with 40 mM KCl (primary islet cells). Mean ± SEM from independent experiments (B; n=3). Statistical significance was determined by 1-way ANOVA with post hoc Tukey multiple comparisons test. \*P<0.05; \*\*P<0.01 and \*\*\*P<0.001.

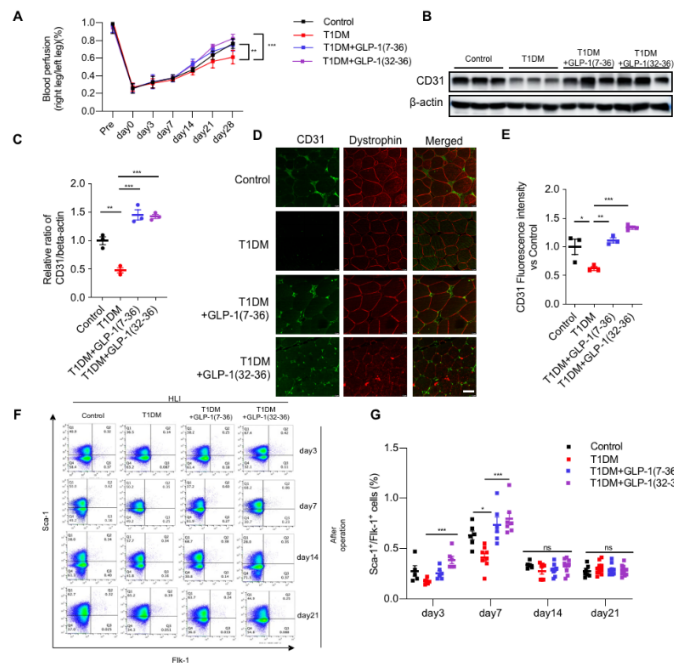


**Figure 2: GLP-1(32-36) improves blood perfusion, angiogenesis, and endothelial progenitor cell mobilization in ischemic hindlimbs of type 1 diabetic mice (T1DM).** The proangiogenic effect of GLP-1 (32-36) in diabetic ischemic tissues was investigated in T1DM mice. GLP-1(7-36) is as a full-length peptide control. (A) blood flow reperfusion was assessed by Doppler laser ultrasound on day 0, 7, 14, and 28 after ischemic injury. The ratio of ischemic/non-ischemic perfusion was quantitatively analyzed ( $n=6$  mice/group). (B-C) CD31 expression in ischemic hind limb by Western blotting.  $\beta$ -actin was used as loading control. (D-E) Anti-CD31 immunostaining in gastrocnemius muscle on day 28 after HLI, showing CD31-positive capillaries per muscle fiber with dystrophin staining ( $n=6$  mice/group, Scale bar: 100  $\mu$ m). (F) EPC (shown as Sca-1<sup>+</sup>/Flk-1<sup>+</sup>cells) mobilization after tissue ischemia in T1DM mice after administration of GLP-1(32-36) was determined by flow cytometry. (G) Percentage of Sca-1<sup>+</sup>/Flk-1<sup>+</sup> cells from different groups (mean  $\pm$  SEM from 6 individual mice per group). Mean  $\pm$  SEM from independent experiments. Statistical significance was determined by 1-way ANOVA with post hoc Tukey multiple comparisons test. \* $P$ <0.05; \*\* $P$ <0.01; \*\*\* $P$ <0.001; ns, no significance.

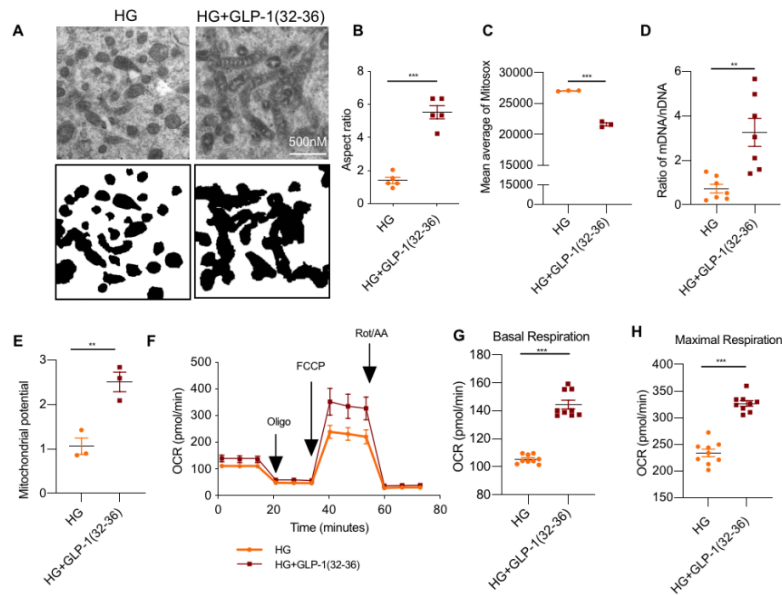


**Figure 3. GLP-1(32-36) rescues mitochondrial dynamics and function of mEPCs.** Mice primary bone marrow EPCs (mEPCs) from T1DM mice or T1DM mice injected with GLP-1(32-36) were isolated and cultured, and the 3- to 5-passage mEPCs were used for further experiments. (A) Representative TEM micrographs of EPCs mitochondria (top panel). Tracing of mitochondria from TEM micrographs (bottom panel). (B) Average aspect ratio for each group from A. (C) Mitochondrial ROS shown as fluorescence intensity of MitoSOX measured by flow cytometry. (D) mtDNA copy numbers relative to nuclear DNA (nDNA) detected by RT-PCR. (E) Mitochondrial membrane potential shown as JC-1 fluorescence ratio between red and green. (F) Sequential oxygen consumption rate (OCR) curve was assessed using the Seahorse XF96 analyzer. (G-H) Representative basal and maximal respiration are shown. Quantification of OCR was calculated. Mean  $\pm$  SEM from independent experiments (B, n=5-7; C, n=3; D, n=7; E, n=3; G&H, n=9). Statistical significance was determined by 1-way ANOVA with post hoc Tukey multiple comparisons test. \*P<0.05; \*\*P<0.01; \*\*\*P<0.001.

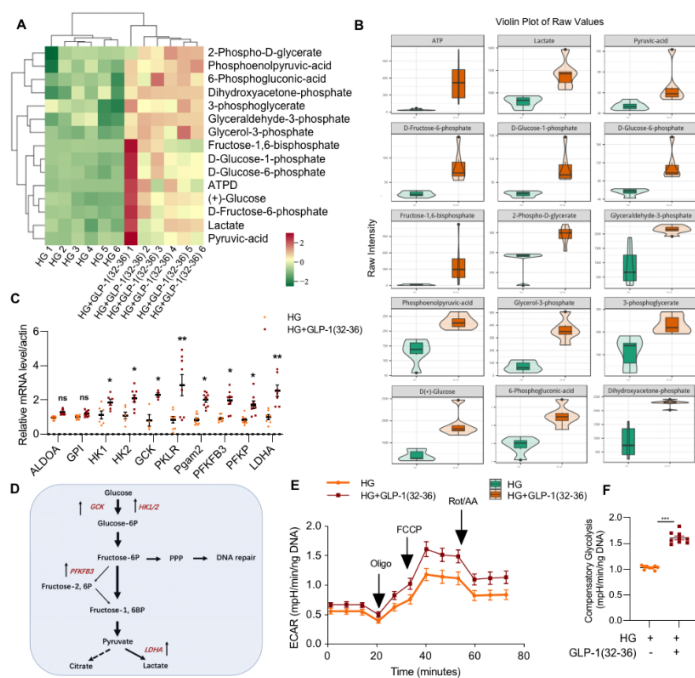


**Figure 4. GLP-1(32-36) facilitates glucose flux through glycolysis and transcription of glycolysis-related genes.** Metabolome analysis of EPC extracted from mouse marrow ( $n=6$ ). The cells were divided into two groups with corresponding treatment (HG vs HG+GLP-1(32-36)). (A) Heatmap of glycolytic related metabolites across all experimental animals of both groups. Red represents high levels and green, low levels. (B) Violin plotting to show data distribution and its probability density, with the box in the middle representing the quartile range; the thin black line extending from it, the 95% confidence interval; the black horizontal line in the middle, the median; and the outer shape, the distribution density of the data. (C) mRNA changes were validated by qPCR of selected glycolytic genes. (D) Upregulation of selected genes within the glycolytic pathway in EPCs from T1DM mice receiving GLP-1(32-36). (E-F) Glycolytic flux (ECAR, extracellular acidification rate using Seahorse XF) in EPCs from two group of T1DM mice ( $n = 9/\text{time point}$ ). Data in C, E and F represent mean  $\pm$  SEM from independent experiments (C&F;  $n=6$ ). Statistical significance was determined by Student's 2-tailed t test. \* $P<0.05$ , \*\* $P<0.01$ ; \*\*\* $P<0.001$ ; ns, no significance.

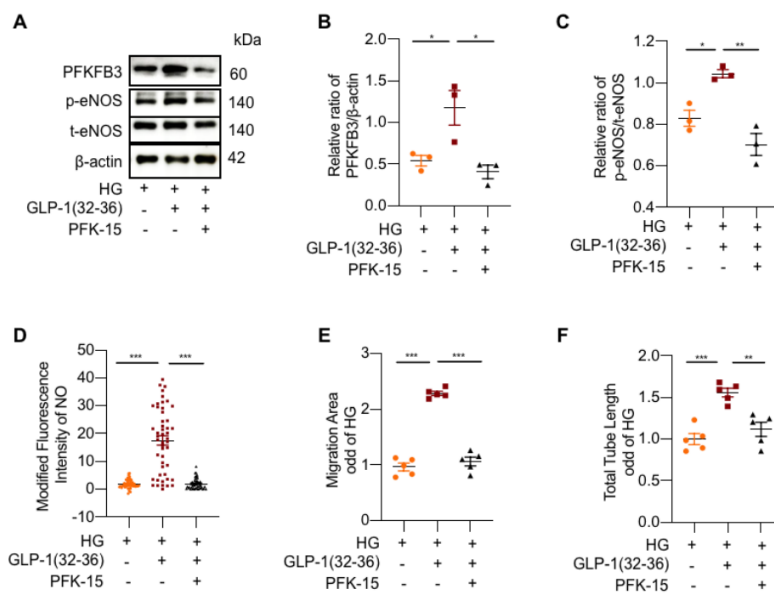


**Figure 5. PFKFB3, a key molecule of glycolysis activator, is involved in regulating GLP-1(32-36)-mediated angiogenesis.** mEPCs isolated from T1DM mice or T1DM mice injected with GLP-1(32-36) were subjected to additional treatment with PFK15, PFKFB3 inhibitor. (A) EPCs extracts were fractionated by SDS-PAGE and analyzed by Western blotting with antibodies to p-eNOS, eNOS and PFKFB3. β-actin was used as protein loading control. (B) Ratio of p-eNOS to eNOS. (C) Ratio of PFKFB3 to β-actin. (D) The production of NO in mEPCs was measured with a DAF-FM diacetate kit. (E) Quantification of the migration area were taken in 5 random microscopy fields per sample. (F) Quantification of the total tube length in tube formation assay. Data were shown as mean ± SEM from independent experiments (B & C, n=8; D, n=40-50; E & F; n=5). Statistical significance was determined by 1-way ANOVA with post hoc Tukey multiple comparisons test. \*P<0.05; \*\*P<0.01; \*\*\*P<0.001.

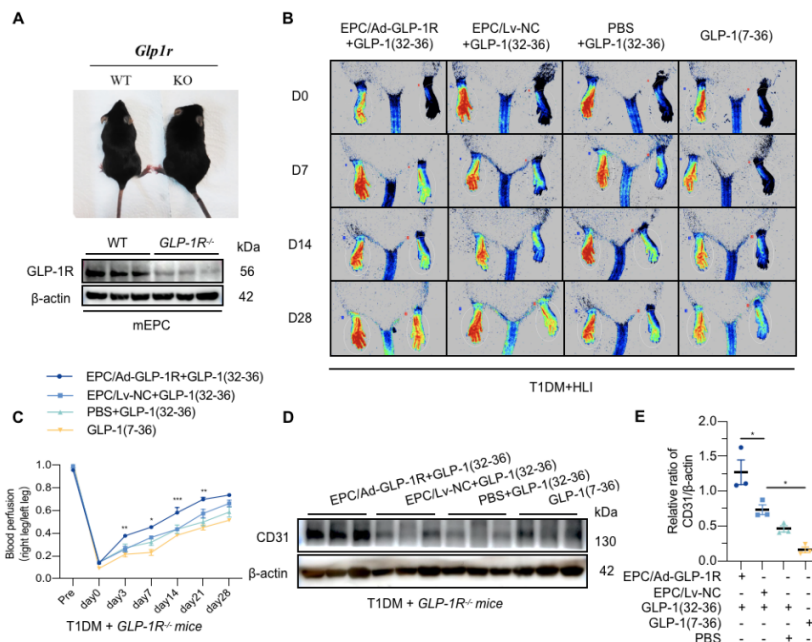


**Figure 6. GLP-1(32-36) depends on the cognate GLP-1R to exert its role in improved blood perfusion and angiogenesis of ischemic limb of T1DM mice.** (A) Mating strategy to generate GLP-1R knockout in diabetic mice and western blotting detected the expression of GLP-1R in WT and KO mice. (B) Representative images showing blood flow reperfusion assessed by Doppler laser ultrasound on day 0, 7, 14, and 28 after ischemic injury. (C) Time courses of blood perfusion shown in images and quantitative analysis after HLI surgery of GLP-1R-/- mice with or without GLP-1R-expressing EPC transplantation in response to GLP-1(32-36) treatment. (D) Western blotting of CD31 expression in gastrocnemius muscle from GLP-1R-/- mice receiving the cell therapy on day 28. β-actin was used as a loading control. The gels shown here are representative of three individual experiments. (E) Ratio of CD31 to β-actin. Data represent mean ± SEM from independent experiments (B-H, n=6-8; J, n=3). Statistical significance was determined by 1-way ANOVA with post hoc Tukey multiple comparisons test. \*P<0.05; \*\*P<0.01, \*\*\* P<0.001; ns, no significance.

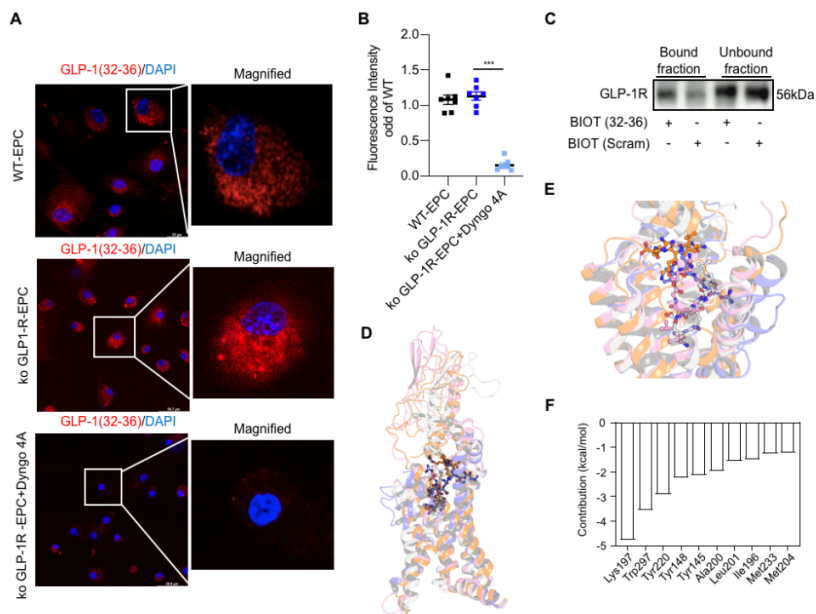


**Figure 7. GLP-1(32-36) binds to GLP-1R without requiring its mediation for entry.** (A) mEPCs isolated from wild-type and *Glp1r*-/- mice were incubated with 100 $\mu$ M Cy5 tagged GLP-1(32-36) with or without dynamin inhibitor Dyng4A (30 $\mu$ M) for 30 (as above) min, and then imaged with spinning disk confocal microscope. (B) Fluorescent intensity of Cy5-GLP-1(32-36) was quantified using ImageJ software. (C) Western blotting analysis of GLP-1R in bound and unbound fractions from pull-down experiments showed preferential binding of GLP-1R to biotinylated GLP-1(32-36) [BIOT (32-36)] as compared with the biotinylated scrambled (32-36) control [BIOT (scram)]. (D) Prediction of the binding mode between GLP-1(32-36) and GLP-1R. Overview of global docking of peptide to 4 crystal structures of GLP-1R (5NX2: light gray, 6ORV: light blue, 6X18: pink, 7C2E: orange). Detailed view of global docking of GLP-1(32-36) to 4 crystal structures of GLP-1R (5NX2: light gray, 6ORV: light blue, 6X18: pink, 7C2E: orange). (F) Top-ranking key residues of GLP-1R in binding with GLP-1(32-36). Data were mean  $\pm$  SEM from independent experiments (B, n=8). Statistical significance was determined by 1-way ANOVA with post hoc Tukey multiple comparisons test. \*P<0.05; \*\*P<0.01; \*\*\*P<0.001.

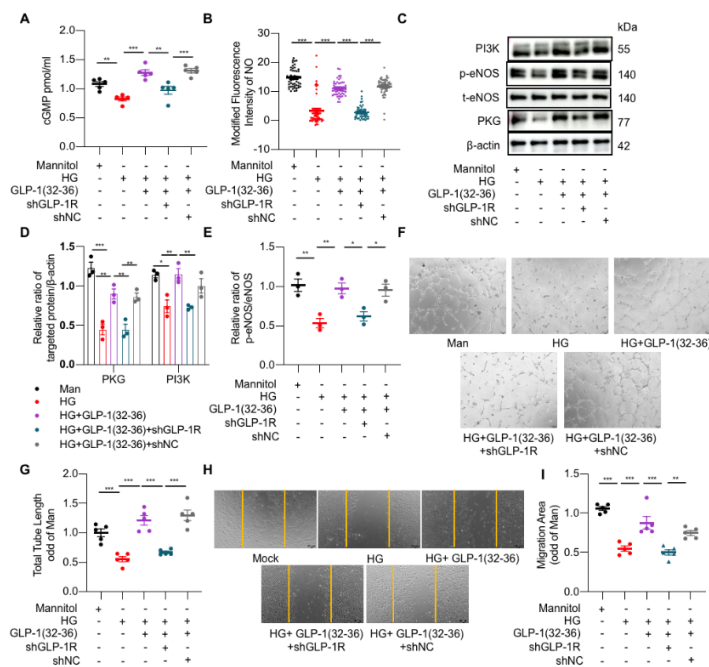


**Figure 8. Both GLP-1(32-36) and GLP-1R are required in improving angiogenesis via the eNOS/cGMP/PKG pathway.** hEPCs were infected with lentivirus expressing shRNA targeting *Glp1r* for 12 h and treated with GLP-1(32-36) (100 nM), and then incubated in high glucose (33 mM) for 24 h. Mannitol (Man) was used as the control. (A) cyclic GMP was detected by using the cGMP ELISA Kit ( $n=5$ ). (B) NO secretion was measured with a diacetate diaminofluorescein-FM (DAF-FM) diacetate kit and was imaged on a fluorescence microscope. (C) EPCs extracts were fractionated by SDS-PAGE and analyzed by Western blotting with antibodies against p-eNOS (Ser1177) and eNOS, PI3K and PKG.  $\beta$ -actin was used as loading control. The gels shown here are representative of 3 individual experiments. (D) Ratio of PKG or PI3K to  $\beta$ -actin (E) Ratio of p-eNOS to eNOS. (F-G) Quantification of the total tube length in EPCs, images of tube morphology were taken in 5 random microscopy fields per sample. (H-I) Quantification of the migration area were taken in 5 random microscopy fields per sample. Scale bars: 500  $\mu$ m. Data were mean  $\pm$  SEM from independent experiments (A,  $n=5$ ; B,  $n=50$ ; D&E,  $n=3$ ; F&G,  $n=5$ ). Statistical significance was determined by 1-way ANOVA with post hoc Tukey multiple comparisons test. \* $P<0.05$ ; \*\* $P<0.01$ ; \*\*\* $P<0.001$ .

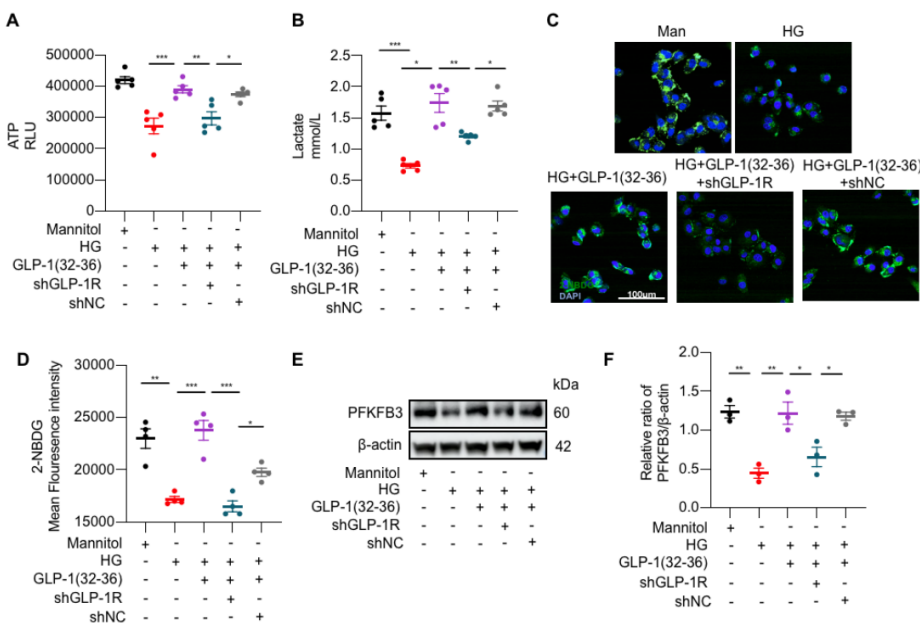


**Figure 9. Both GLP-1(32-36) and GLP-1R are involved in regulating PFKFB3-mediated glycolysis.** hEPCs were infected with the lentivirus expressing shRNA targeting *Glp1r* for 12 h and treated with GLP-1(32-36) (100 nM), and then incubated in high glucose (HG, 33 mM) for 24 h. Mannitol (Man) was used as the control. (A) ATP content. (B) Lactate production. (C-D) Uptake of 2-NBDG as determined by immunofluorescence staining and flow cytometry analysis. (E) EPCs extracts were fractionated by SDS-PAGE and analyzed by Western blotting with PFKFB3. β-actin was used as loading control. (F) Ratio of PFKFB3 to β-actin. The gels shown here are representative of 3 individual experiments. Data are expressed as mean ± SEM from independent experiments (A, n=5; B, n=6; D, n=4; F, n=3). Statistical significance was determined by 1-way ANOVA with post hoc Tukey multiple comparisons test. \*P<0.05; \*\*P<0.01; \*\*\*P<0.001.